9th International Conference on Fracture Mechanics of Concrete and Concrete Structures
FraMCoS-9
V. Saouma, J. Bolander, and E. Landis (Eds)

DOI 10.21012/FC9.053

INFLUENCE OF MOISTURE AND TEMPERATURE ON MECHANICAL PROPERTIES OF THE CONCRETE

H. KALLEL[*†], H. CARRE[*], C. LABORDERIE[*], B. MASSON[†] AND N.C. TRAN[‡]

[*]University of Pau and Pays de ladour
Anglet, France
e-mail: hatem.kallel@univ-pau.fr
e-mail: helene.carre@univ-pau.fr
e-mail: christian.laborderie@univ-pau.fr

[†]Electricité de France (EDF), R&D
Moret sur Loing, France
e-mail:benoit.masson@edf.fr

[‡]Electricit de France (EDF), SEPTEN
Villeurbanne, France
e-mail: nhu-cuong.tran@edf.fr

Key words: Concrete, Temperature, Pressure, Water Content, Fracture Energy, Modulus of Elasticity, Tensile strength

Abstract. The scenario of a severe accident in the containment building of a nuclear plant results in an increase in pressure, temperature and relative humidity that can reach respectively 5 bars, 140 C and the water vapour saturation. Accurate knowledge of the thermal and mechanical behaviour of materials and more specifically of concrete is required to carry out more precise numerical simulations, in order to be able improve the precision of regulatory calculations.

Our study aims to investigate the mechanical behaviour of concrete under homogeneous conditions of moisture and temperature. An experimental apparatus was designed in order to assess the evolutions of the fracture energy, the modulus of elasticity and the traction resistance of concrete. Different temperature levels up to a maximum of 140 C and at different values of the controlled moisture content were investigated. The equipment was used to perform DCT (Disk-shape Compact Tension) tests at 30, 90, 110 and 140 C. Five levels of degree of liquid water saturation (S_w) were investigated for each temperature level between 36 and 100 %.

1 INTRODUCTION

Measurements of the mechanical properties of concrete under controlled conditions of temperature but without control of relative humidity [1–4] and mechanical tests under different percentages of degree of saturation and controled temperature exist in literature [5, 6]. To our knowledge, in literature, there are no measurements of the mechanical properties of concrete under controlled conditions of temperature and relative humidity except the results of Bazant [7] who measured the strength of concrete at dry state and at 100 % of relative humidity at different levels of temperature.

It is interesting to study the evolution of the mechanical properties of concrete in dependence of temperature and degree of saturation. But in order to regulate the relative humidity at temperatures higher than 100 °C, it is necessary

to take into account the pressure. In fact, these three parameters (temperature, degree of saturation and pressure) influence on the evolution of fracture energy, elastic modulus and traction resistance. Thus, their combination must beinvestigated.

The objective of this experimental work is to characterise the evolution of the fracture energy, the modulus of elasticity and the tensile strength in function of temperature, degree of saturation (S_w) and pressure. For this purpose, the DCT tests (Disk-shape Compact Tension) [8, 9] has been chosen to determine this evolution. The DCT tests have been performed under hydrothermal controlled conditions. The different degree of saturation in liquid water, S_w are obtained by be storing the specimens in an environment at imposed relative humidity. The target values of degree of saturation are the following: 36, 56, 68, 96 et 100 %. The temperature has been fixed at four target values : 30, 90, 110 and 140 °C. This choice allows to measure the influence of temperature on the behaviour of concrete by considering the temperature under service condition and under a severe accident in a confinement reservoir in a nuclear plant. For temperatures of 110 and 140 °C, the pressures of the saturated vapour are respectively 1.4 and 3.5 bar.

2 Materials and specimens

2.1 Formulation and characteristics

An ordinary concrete called BMacena, representative of the concretes used for French nuclear power plants, was chosen. Its composition is presented in Table 1.

Table 1: Concrete mix

BMacena	Quantity (kg/m^3)
CEM I 52,5 N CE CP2 NF (Gaurain)	320
Sand 0/4 (Varennes)	830
Gravel 4/11 (Varennes)	445
Gravel 8/16 (Balloy)	550
Superplasticizer SIKAPLAST 80	2.75
Total water	197.6
E/C	0.62

The standard mechanical properties of the hardened concrete at 28 and 90 days are reported in Table 2. These properties were obtained by calculating the mean value of two samples performed on 16 x 32 cm specimens. Tensile strength was evaluated using the splitting test.

Table 2: Standard characteristics of hardened concrete NF EN 12390

	Compressive strength f_c (MPa)	Tensile strength f_t (MPa)	Modulus of elasticity E (GPa)
28 days	41	3.7	32.2
90 days	43	4.2	-

2.2 Specimens

In this study, the DCT specimen [9] is used (see Figure 1). Letter D indicated that the specimen is a disk, letter C indicates that the specimen is compact and letter T indicates that the load is applied in traction. The principle of this test is simple: it consists in submitting the specimen to an increasing tension or to a constant displacement until failure. During the test, the crack opening and the applied load are recorded by means of a data logger system. The DCT test is generally used to test samples of steel [10] and asphalt [11], but we used the DCT test on concrete because the samples have a specific geometry that allows to reduce the volume under pressure during the test.

In this study, the principle of the DCT tests can be used for the whole experimental campaign with the objective of determining the parameters E, F_t and G_f.

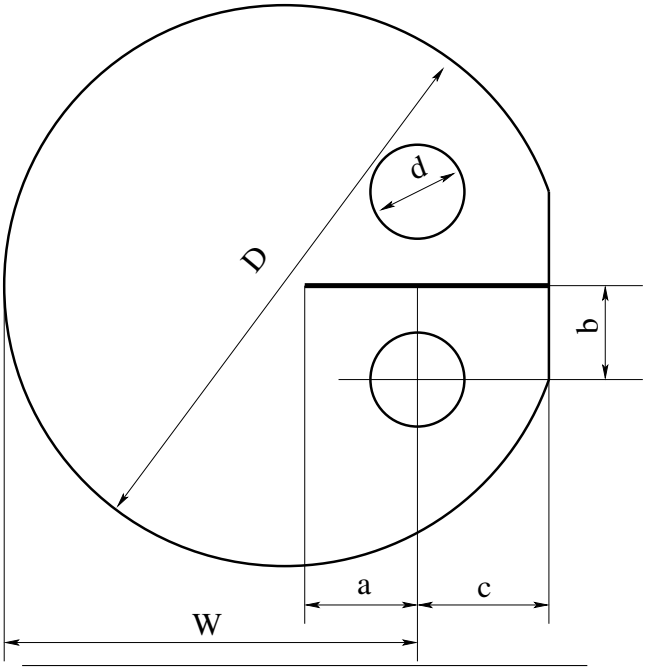

D	W	a	b	c	d	thickness
150	110	30	25	35	25	50

Figure 1: DCT Specimen

2.3 Hydro-thermal balancing of specimens

After demoulding, the specimens are stored in water at 20 °C and they are considered fully saturated at the beginning of the equalisation process. A series of specimens is kept in water and for the other ones, the equalisation starts 90 days after the mixing of the concrete. In order to accelerate the desaturation process and the equalisation of our specimens, it has been decided to store specimens at 60 °C except for a series. Furthermore, in order to perform the test in a reasonable time, we needed to keep different specimen in different environments at the same time. We used salt solutions to regulate the different levels of relative humidity.

The saturated salt solutions were disposed at the bottom of the containers (Table 3). The relative humidity is regularly controlled by a thermo-hygrometer capable of measuring relative humidity that ranges from 10 % to 98 % . Three specimens are placed in each container and for each level of relative humidity, we used two containers that later have been placed in an oven in which temperature was increased with a rate of 1 °C/min up to 60 °C.

Table 3: RH values obtained from different salt solutions

	1	2	3	4
Salt solution	KCL	KNO3	K2SO4	K2SO4
Temperature	60	60	60	20
Theorical R.H.	81 %	85 %	95 %	98 %
Measured R.H.	83 %	93 %	98 %	98 %

At this stage, all specimens are placed in their environment. Some specimens were weighed regularly, in order to establish if stabilisation is completed and to determine the isothermal desorption of the material.

The surface of the specimens is wiped if necessary. The measurements are performed in a very short time and always by respecting the procedure whose effect is considered negligible on hydro-thermal state. The weight is measured by using a scale with a precision of 0.01 g.

The control of the equilibrium was done by regularly checking the evolution of the mass of all samples (Figure 2). We supposed that the equilibrium is attained when the mass of the specimen changes less than 0.1 % between two measurements over a week. The control on the masse was done on three samples for each environment. Figure 2 represents the curves that correspond to one of the specimens for each environment.

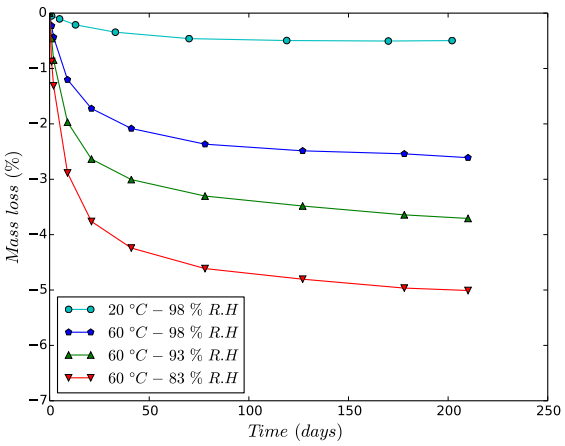

Figure 2: Relationship between material mass loss and current time for DCT test

Table 4 shows the degree of water saturation of samples at equilibrium in their corresponding environment. This table also shows the observed balancing times for the different environments.

Table 4: Water saturation percentages for DCT specimens

Environment	1	2	3	4
S_w	31 37	50 51	63 65 68	93 93 94 94
Average	34 -3/+3%	51 -1/+0%	65 -2/+3%	94 -1/+0%
Balancing time (j)	490 jours	490 jours	490 jours	490 jours

3 DCT test equipment

In order to maintain humidity in the atmosphere for temperature higher than 100 °C, it is necessary to apply pressure. For this reason, we built a new experimental device (called pressurized cell) in which we performed the mechanical tests (DCT tests) under controlled conditions of temperature (up to 140 °C) and pressure (up to 4 bars).

The experimental device respect specific requirements such as:

- Evolution of degree of saturation in specimens must ne neglectable during testing
- Pressure of 4 bars can be reached in the pressurized cell
- The pressurized cell must be sealed to air and water
- The measurements of displacement and load must be logged during testing and hence all transducers must support testing conditions

The pressurized cell contains a water tank with an electrical resistance (Figure 3). The resistance is controled with a thermocouple located close to specimen. When the temperature in water exceeds 100 °C, water evaporates and pressure increases. A pressure valve is used to release air to obtained precisely the target value. During the test, air is saturated of water vapour. In prelimlinary tests, specimens have be weighted before and after heating. The increase of weigth is less than 0.01 % for a degree of saturation of 36 %. This is considered neglectable. Two stainless steel rollers were used for application of the load. Two stainless steel helmets were linked to the rollers and to the hydraulic press.

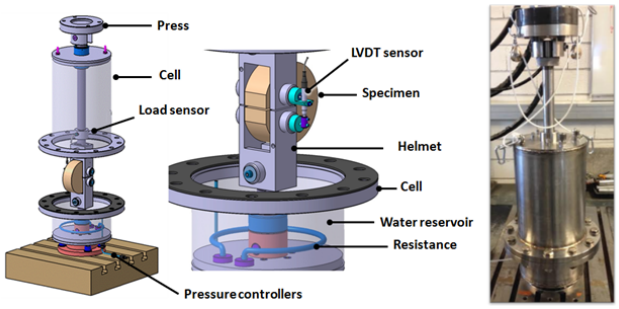

Figure 3: Test device

4 Experimental analysis

4.1 Fracture energy

Fracture energy was assumed to be the total work of the applied load by unit of crack area:

$$G_f = \frac{W_0}{A_{lig}}$$

Where
G_f: fracture energy [N.m^{-1}]
W_0: work applied of the applied load [N.m]
A_{lig}: area of the unnotched part of the specimen (plane fracture area at the end of the test) [m^2]

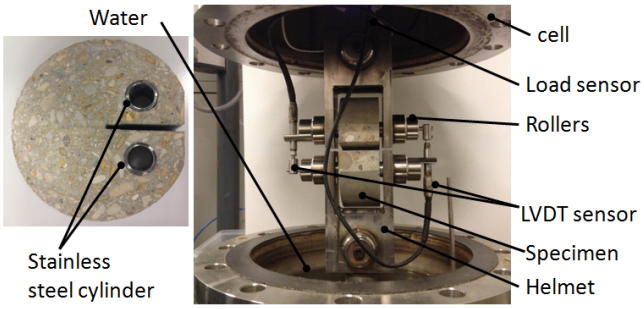

Figure 4: DCT test

4.2 Modulus of elasticity

In order to determine the elastic modulus by means of a DCT test, we performed a numerical calculation to determine the relation between the real elastic modulus and the slope of the initial curve between force and relative rollers displacement. Then, the equation 1 can be used to determine the modulus of elasticity

$$E_{exp} = E_0 \frac{K_{exp}}{K_0} \tag{1}$$

Where
E_0 = 30 GPa modulus of elasticity used for the numerical calculation
K_{exp} = experimental slope
K_0 = 14.90 KN/m

4.3 Tensile strength

The tensile strength of concrete is usually deduced from the peak load. In most cases this is not completely true and softening of concrete begins before the peak, which therefore depends on the elastic and softening characteristics of the material. We assume in the following that the softening of concrete in tension can be correctly depicted by means of a coupled elastoplastic damage model that uses a crack band approach. The model initially developed by Fichant et al. [12] was recently modified in order to better take into account the fracture energy [13]. It is implemented in the recent versions of Cast3M [14] and known as "MICROISO". In the event of slow loading, the results of simulations depend only on 3 parameters: modulus of elasticity E, fracture energy G_f and tensile strength f_t, assuming that the Poisson's ratio ν is known (a standard value of $\nu = 0.2$ is hereby taken). Assuming that the values of the modulus of elasticity and of the fracture energy are known, the peak load becomes a function depending on the unique value of the strength f_t. A first computation is performed with a start value of $f_{t_1} = 1.8MPa$, then the maximum value of the computed load F_{M_i} is compared to the experimental value $F_{M_{exp}}$ and a new computation is performed with a new value of f_t corrected by a Newton Raphson method.

$$f_{t_{i+1}} = f_{t_i} + \frac{((F_{M_{exp}} - F_{M_i}) * (f_{t_i} - f_{t_{i-1}})}{F_{M_i} - F_{M_{i-1}}} \tag{2}$$

The load displacement curves obtained during the iterative process are reported in Figure 5. 5 iterations allowed us to obtain a good approximation.

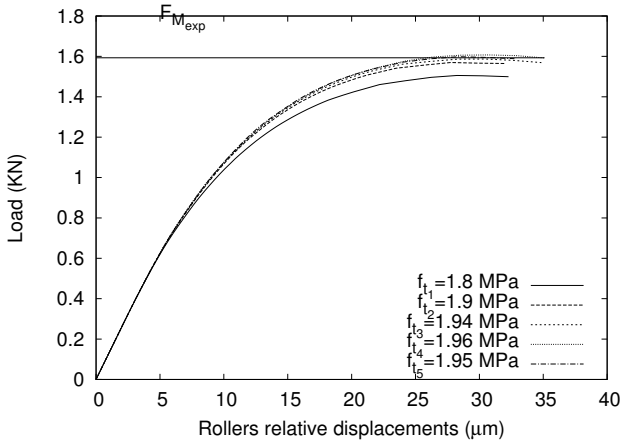

Figure 5: Iterative process for the determination of tensile strength f_t

The computation performed with the identified parameters (E, f_t and G_f) is compared to experimental results in Figure 6. A good agree-

ment between numerical simulations and experimental results can be observed.

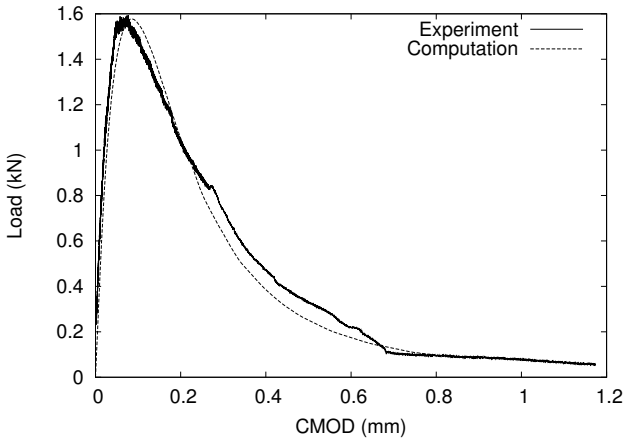

Figure 6: Computation with identified parameters

5 Results and discussion

5.1 Fracture energy under controlled temperature and relative humidity

Table 5 shows the different fracture energy results obtained using the DCT test. Tests were performed at temperatures of 30, 90, 110 °C and 140 °C , at different relative humidity values as described above, corresponding to different values of S_w and different pressure.

Fracture energy depends on the degree of water saturation for the samples tested at 30, 90, 110 °C and at 140°C Figure 7. For 30 and 90°C, fracture energy decreases linearly as the degree of water saturation increases but does not seem to be affected by the temperature. The results are in good agreement with the results obtained by Bazant [7].

The increase in G_f with the decrease in S_w can be explained by the capillary pressure, which increases as S_w decreases. This induces local compressive stresses between the pores. Because of these compressive stresses, the propagation of cracks is harder and greater energy is necessary for the creation of cracks. For 110 and 140 °C, the results are very close even if the values obtained at 110°C are slightly higher than the values obtained at 140 °C. G_f increases linearly with S_w.

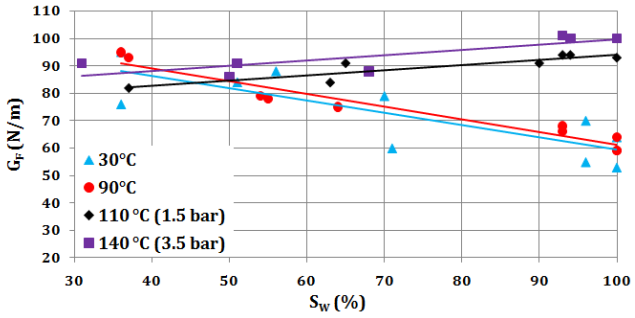

Figure 7: Evolution of fracture energy with the degree of water saturation at 30, 90, 110 °C (1.4 bar) and at 140°C (3.5 bar).

Table 5: Evolution of fracture energy with the degree of water saturation at 30, 90, 110 °C (1.4 bar) and at 140 °C (3.5 bar)

G_f (N/m)			
S_w	30 °C	S_w	90 °C
37	82	31	91
63	84	50	86
65	91	51	91
90	91	68	88
93	94	93	101
94	94	94	100
100	93	100	100

G_f (N/m)			
S_w	110 °C	S_w	140 °C
37	82	31	91
63	84	50	86
65	91	51	91
90	91	68	88
93	94	93	101
94	94	94	100
100	93	100	100

5.2 Elastic modulus under controlled temperature and relative humidity

Table 6 and Figure8 gives the results of the elastic modulus obtained from the DCT tests and finite element computations.

Except fo 90°C, the modulus of elasticity is almost constant between 36 and 95 %. An increase in the elastic modulus was registered as the degree of saturation increased from 95 %

to 100 %. The results at 30°C agrees with the those obtained by Chen [15] who explained this phenomenon by the saturation of the biggest pores. The low compressibility of water induces fewer deformations of the pores and a higher modulus of elasticity.

Table 6: Evolution of Elastic modulus with the degree of water saturation at 30, 90, 110 °C (1.4 bar) and at 140 °C (3.5 bar)

E (GPa)			
S_w	30 °C	S_w	90 °C
36	25	36	26
51	21	54	16
71	23	65	16
96	21	93	18
96	34	93	15
100	28	100	20
100	32	100	23

E (GPa)			
S_w	110 °C	S_w	140 °C
37	31	31	36
63	40	50	36
65	32	51	38
90		68	40
93	41	93	48
94	56	94	56
100	53	100	58

5.3 Tensile strength under controlled temperature and relative humidity.

The evolution of the Tensile strength with S_w is shown in Figure 9 and Table 7. It can be observed that the tensile strength is practically constant while the degree of saturation changes from 36 % to 68 %. An increase of the tensile strength has been observed while the degree of saturation increases from 68 % to 100 %.

The drying of concrete induces a shrinkage in the cement paste but not in the aggregates. This mismatch leads to the appearance of cracks at the interface between cement paste and the aggregates. This can facilitate the appearance of the first macroscopic crack and the decrease in tensile strength.

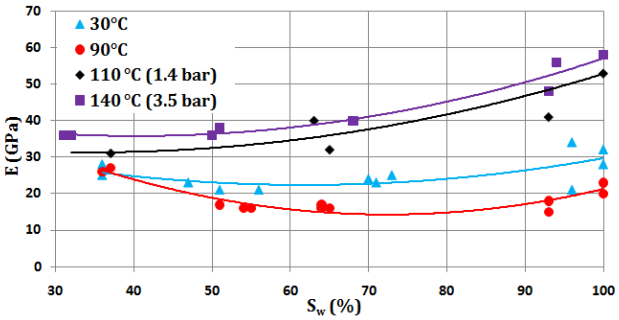

Figure 8: Evolution of Elastic modulus with the degree of water saturation at 30, 90, 110 °C (1.4 bar) and at 140 °C (3.5 bar).

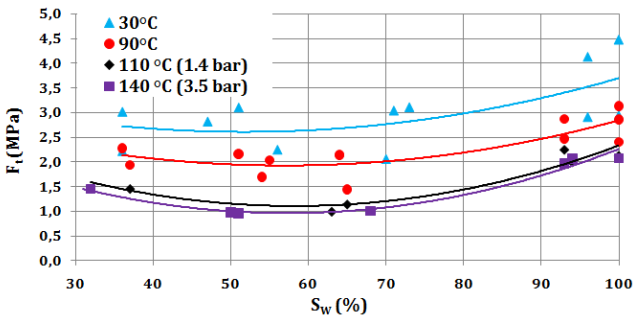

Figure 9: Evolution of the Tensile strength with the degree of water saturation at 30, 90, 110 °C (1.4 bar) and at 140 °C (3.5 bar).

Table 7: Evolution of Tensile strength with the degree of water saturation at 30, 90, 110 °C (1.4 bar) and at 140 °C (3.5 bar)

F_t (MPa)			
S_w	30 °C	S_w	90 °C
36	2.23	36	1.95
51	3.11	54	1.70
71	3.05	36	2.14
96	2.91	93	2.47
96	4.13	93	2.877
100	2.95	100	2.86
100	4.84	100	3.14

F_t (MPa)			
S_w	110 °C	S_w	140 °C
37	1.46	31	1.45
63	1.00	50	0.98
65	1.15	51	0.96
90		68	1.00
93	2.25	93	1.97
94	2.00	94	2.06
100	2.13	100	2.08

6 CONCLUSIONS

The evolutions of Young's modulus E, Fracture energy G_f and tensile strength F_t were measured at different values of the degree of water saturation for temperatures ranging from 30°C to 140 °C. A specific vessel was designed in order to perform experiments under autoclave vapour condition for temperatures higher than 100 °C. The first results show that:

At constant and homogeneous values of S_w.

- F_t decreases monotonously with the temperature and can be divided by two between 30°C and 140 °C.
- E slightly decreases between 30°C and 90°C and then increases for temperatures greater than 100 °C
- G_f increases with the temperature, the relative increasing is as more important for high values of the saturation degree.

At constant values of temperature

- F_t and E remain nearly constant when S_w ranges from 30 % to 60 % and then increase when S_w ranges from 60 % to 100 %
- G_f decreases with S_w when the temperature is lower than 100 °C and a conversely increases with S_w for higher temperatures.

Some physical explanations could be found for each individual result, but at first glance some of them seems to be antagonist.Thermo-Hygro-Mechanical Numerical computations performed at the meso-cale may help to better understand these experimental results.

REFERENCES

[1] Izabela Gaweska-Hager. *Comportement à haute température des bétons à haute performance - évolution des principales propriétés mécaniques*. Phd thesis, École Nationale des Ponts et Chaussées & École Polytechnique de Cracovie, November 2004. In french.

[2] Dominique Kalifa, Pierre & Menneteau. Mesures de pression, tempratures et perte en masse dans les btons hautes tempratures. Technical report, CSTB, 1999.

[3] Hisham Abdel-Fattah and Sameer A. Hamoush. Variation of the fracture toughness of concrete with temperature. *Construction and Building Materials*, 11(2):105–108, March 1997.

[4] Hélène Carré and Pierre Pimienta. Bending tests at higth temperatures. In *ICEM15,* 15^{th} *International Conference on Experimental Mechanics*, page #3802, Porto, Portugal, 22-27 July 2012.

[5] Sandor Popovics. Effect of curing method and final moisture condition on compressive strength of concrete. *Journal Proceedings*, 83(4):650–657, January 1986.

[6] Flore Brue, Catherine A. Davy, Frdric Skoczylas, Nicolas Burlion, and Xavier Bourbon. Effect of temperature on the water retention properties of two high performance concretes. *Cement and Concrete Research*, 42(2):384396, Feb 2012.

[7] Zdenek P. Bažant and Pere C. Prat. Effect of temperature and humidity on fracture energy of concrete. *ACI Materials Journal*, 85(4):262–271, July 1988.

[8] A. Amirkhanian, D. Spring, J. Roesler, K. Park, and G. Paulino. Disk-shaped compact tension test for plain concrete. In *Transportation and Development Institute Congress*, pages 688–698, Chicago, Illinois, United States, March 13-16 2011. ASCE.

[9] D04 Committee. Test Method for Determining Fracture Energy of Asphalt-Aggregate Mixtures Using the Disk-Shaped Compact Tension Geometry. Technical report, ASTM International, 2013.

[10] Julie Cummings. étude de la propagation de fissures dans les sols granumlaires gelés. Master's thesis, University of Laval (Canada), 2000.

[11] Hyunwook Kim, Michael P. Wagoner, and William G. Buttlar. Numerical fracture analysis on the specimen size dependency of asphalt concrete using a cohesive softening model. *Construction and Building Materials*, 23(5):21122120, May 2009.

[12] Stphanie Fichant, Gilles Pijaudier-Cabot, and Christian La Borderie. Continuum damage modelling : Approximation of crack induced anisotropy. *Mechanics Research Communications*, 24(2):109–114, 1997.

[13] Mohammed Matallah, Christian La Borderie, and Olivier Maurel. A practical method to estimate crack openings in concrete structures. *International Journal for Numerical and Analytical Methods in Geomechanics*, 34:1615–1633, 2010.

[14] CEA. Cast3m finite element code. Technical report, French Alternative Energies and Atomic Energy Commission.

[15] Da Chen. *Modélisation du comportement hydromécanique d'un mortier sous compression et dessiccation*. PhD thesis, University of Lille (France), 2005.